Optics Letters

2 MW peak power generation in fluorine co-doped Yb fiber prepared by powder-sinter technology

Martin Leich,[1,*] André Kalide,[1] Tina Eschrich,[1] Martin Lorenz,[1] Adrian Lorenz,[1] Katrin Wondraczek,[1] Dörte Schönfeld,[2] Andreas Langner,[2] Gerhard Schötz,[2] and Matthias Jäger[1]

[1]Leibniz Institute of Photonic Technology, Albert-Einstein-Straße 9, 07745 Jena, Germany
[2]Heraeus Quarzglas GmbH & KG, Quarzstr. 8, 63450 Hanau, Germany
*Corresponding author: martin.leich@leibniz-ipht.de

Received 9 April 2020; revised 29 May 2020; accepted 4 June 2020; posted 8 June 2020 (Doc. ID 394793); published 4 August 2020

We report on the first, to the best of our knowledge, implementation of a fluorine co-doped large-mode-area REPUSIL fiber for high peak power amplification in an ultrashort-pulse master oscillator power amplifier. The core material of the investigated step-index fiber with high Yb-doping level, 52 μm core and high core-to-clad ratio of 1:4.2 was fabricated by means of the REPUSIL powder-sinter technology. The core numerical aperture was adjusted by fluorine codoping to 0.088. For achieving high beam quality and for ensuring a monolithic seed path, the LMA fiber is locally tapered. We demonstrate an Yb fiber amplifier with near-diffraction-limited beam quality of $M^2 = 1.3$, which remains constant up to a peak power of 2 MW. This is a record for a tapered single core fiber.

https://doi.org/10.1364/OL.394793

Introduction. Fiber amplifiers contribute to a variety of applications in material processing due to their outstanding beam quality, performance and flexibility. For remote processes, e.g., structuring large surfaces, a high beam quality, and notably high peak power, are decisive.

Several approaches have been proposed to achieve high power fiber lasers and amplifiers with excellent beam quality. For achieving high peak power nonlinear processes, such as stimulated Raman scattering (SRS) or four-wave mixing (FWM) has to be avoided. For this purpose, specialty fibers with a large effective mode area (LMA) are designed. To reduce the number of guided or amplified modes and therefore to achieve high beam quality, several concepts have been proposed in the literature: single-mode operation was demonstrated on chiral coupled-core fibers with 55 μm core diameter [1] and on a 50 μm core leakage channel fiber with flat-top profile [2]. Other fiber designs that suppress higher order modes are Bragg fibers [3] and the most commonly used to achieve high peak power and diffraction-limited beam quality: photonic crystal fiber (PCF), e.g., in different large-pitch designs [4,5]. Another straightforward approach to realize highly brilliant LMA amplifiers is achieved by adiabatic tapering of multimode step-index fibers. This approach has so far been used to implement a monolithic beam source for peak power scaling close to the megawatt range [6,7].

For achieving high peak power, short fibers with large mode areas are essential. Furthermore, high pump absorption and therefore short fiber lengths are preferred in such fibers requiring high Yb concentrations and large core-to-clad diameter ratios. To achieve high beam quality at the same time, it is necessary to realize a very homogenous refractive index profile (RIP) with low numerical aperture (NA) of the core. The low core NA conflicts with the desired high Yb concentration of the core that intrinsically results in an increase of the refractive index (RI). In presence of other dopants, which are necessary to suppress photodarkening (PD), e.g., aluminum and cerium [8,9], the refractive index is increased even further.

One possibility to reduce the effective core-NA is the implementation of a pedestal design, which can be realized by Ge- or Al-doping [10,11]. Another approach is the direct reduction of the refractive index (RI) of the core glass, e.g., by fluorine codoping of fused silica [12–14]. In [14], it is shown that even fluorine itself can have a significant influence on PD losses of the core glass. Recently, a sol-gel fabricated PCF fiber with F/Yb^{3+} doping was presented [15]. The RI of the core material was adjusted by C_2F_6 to $\Delta n = -4 * 10^{-3}$ with respect to fused silica (F300) and thus only suitable for light guiding in a PCF fiber with 8.6 μm core diameter. A low attenuation of 66 dB/km and high laser efficiency of 70% were demonstrated, but output power was limited to 133 mW. In [16], Xu *et al.* report on an $Yb^{3+}/Al^{3+}/F^-$ codoped silica fiber fabricated by the sol-gel process with 50 μm core diameter and a notably low NA of 0.02. A high beam quality with $M^2 < 1.1$ was demonstrated by bending a 6 m long fiber to 0.35 m diameter; however, the slope efficiency was reduced to 30%–43% due to the high background and bending loss. One technology that meets the requirements for high homogeneity of the dopants and the refractive index profile, that ensures cost-efficient production,

and that is also suitable for the incorporation of high fluorine concentrations into the fiber core material, is the reactive powder-sinter technology (REPUSIL) [17,18].

In this Letter, we report on the first implementation of fluorine codoping combined with REPUSIL technology for fabricating a step index LMA fiber for peak power scaling in a picosecond master oscillator power amplifier (MOPA). Based on this new core material, we have developed a step-index fiber with high Yb-concentration and high core-to-clad ratio of 1:4.2 for greatly increased pump absorption.

To achieve near diffraction-limited beam quality by preferential excitation of the fundamental mode and to ensure a monolithic seed path, the LMA fiber was locally tapered [7]. The NA of the fiber core had to be matched to the single mode delivery seed fiber of the amplifier system ensuring proper mode field matching of the fundamental mode of the tapered LMA fiber. The core NA of the LMA fiber was adjusted by F codoping [14] of the REPUSIL core glass. The principal design of such step index fiber with fluorine codoped and Yb/Al doped core material and its corresponding refractive index profile is shown in Fig. 1.

Preform and fiber fabrication. The LMA fiber preform was fabricated in multiple steps: First, the silica-based core material is produced by reactive powder sinter technology (REPUSIL). This fabrication route has already been described in [17,18]. The powder was doped with 0.28 mol% Yb_2O_3, 1.5 mol% Al_2O_3, and 0.17 mol% Ce_2O_3 for efficient photodarkening suppression. After doping and drying, the powder is compressed into a green body and fluorinated for refractive index reduction [14].

The thermodynamics of fluorine incorporation into silica glass is described in [19]. Online FT-IR monitoring of fluorination evidenced different kinetic phases [20], thus providing a useful tool for efficient process control. The samples were fluorinated in a quartz tube reactor at temperatures ranging from 900°C–1000°C (Carbolite, Folding tube furnace, VST12 600) monitored by online FTIR analysis (Nicolet, FTIR Spectrometer, iS10) of the gas effluents. After several cleaning steps, the fluorinated green body is sintered and vitrified followed by a homogenization step. The core preform is then ground and polished into a cylindrical shape. The resulting active-doped core rod is then jacketed with an F300 silica tube and ground in octagonal shape for serving as a pump cladding.

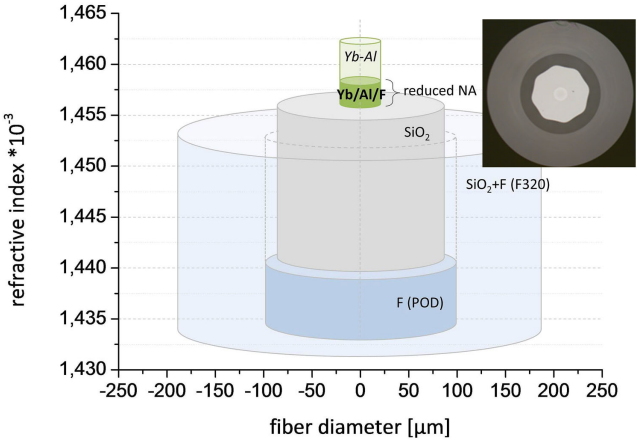

Fig. 1. Fiber design with refractive index compensation by F-codoping.

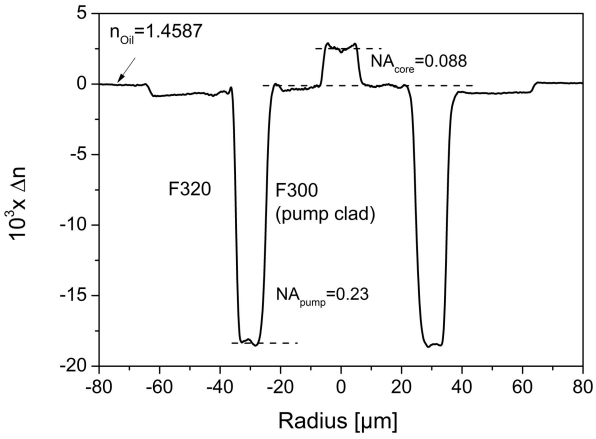

Fig. 2. 1D refractive index profile of REPUSIL fiber.

To ensure guidance of the pump light in this inner cross section of the future fiber, a high-F-containing plasma deposited glass layer (POD) is produced thereon. An additional outer cladding is added, consisting of a slightly F-doped silica tube (F320) to reduce the glass viscosity and therefore allowing to match the drawing temperature of the fiber and taper [7,21]. A scheme of the preform structure is shown in Fig. 1. The preform has been drawn into fiber with 600 µm outer diameter, 220 µm pump cladding diameter, and 52 µm core diameter (Fig. 1, inset). Additionally, a test fiber with 8.5 µm core diameter was drawn for characterization purposes. Fibers were coated with low RI fluorinated acrylate for mechanical protection and power stability.

Fiber characterization and tapering. Dopant concentrations of the core material have been confirmed by electron probe micro analysis (EPMA) at a large core diameter fiber sample with 0.28 mol% Yb_2O_3, 1.5 mol% Al_2O_3, 0.18 mol% Ce_2O_3, and 0.8 mol% SiF_4. Fiber attenuation was determined by means of a high-resolution optical time-domain reflectometer (OTDR) LOR-220 (Luciol Instruments SA) at 1310 nm resulting in 30 dB/km for a 62 m long fiber with 52 µm core diameter.

The refractive index profile (RIP) of the fiber was measured in two dimensions with an IFA-100 optical fiber analyzer (Interfiber Analysis, LLC). For an overview measurement, a sample of the 8.5 µm core test fiber was used. To perform a more accurate measurement of the core region and to improve measurement resolution, the 52 µm core LMA fiber was etched down to an outer diameter of <200 µm. A 1D plot of the RIP measurement of the entire fiber cross section (125 µm fiber) is shown in Fig. 2. The measured core NA with NA = 0.088 is quite well-matched to the seed fiber of the amplifier system with an NA of 0.08. The separately measured 2D core region of the etched fiber is shown in Fig. 3(a). It is assumed that the occurrence of a sharp index peak at the interface between the core and the pump clad is partly related to the intrinsic fiber stress [22] and out-diffusion of fluorine, but also a reduction of SiO_2 during core material production [23] cannot be excluded. In addition, the RI distribution of the fiber core shows a slight index decrease near the center (Fig. 3).

Resulting from numerical simulations (COMSOL Multiphysics), the influence of the RI peaks on the calculated fundamental mode field diameter (MFD) is negligible. However, the RIP of the fiber core shows a slight index decrease

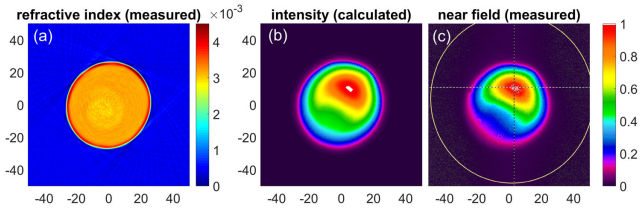

Fig. 3. Measured 2D refractive index profile: (a) simulated, (b) measured, and (c) intensity distribution of the fundamental mode.

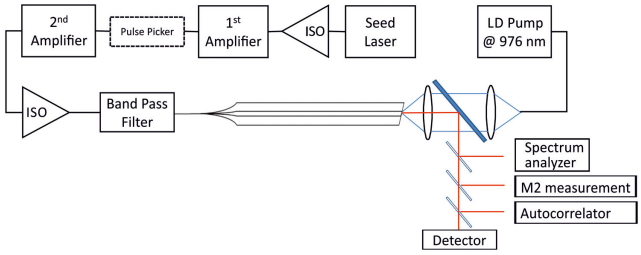

Fig. 4. Picosecond MOPA for peak power scaling.

of about $\Delta n \approx 5 \times 10^{-4}$ near the center [Figs. 2 and 3(a)], which clearly impacts the intensity distribution of the fundamental mode and results in a kidney shape [Fig. 3(b)]. This simulation result was confirmed by measuring the near-field intensity at the output of an adiabatically tapered fiber [Fig. 3(c)].

Tapering of a 0.9 m fiber sample at one end to a core diameter of 8.5 μm was performed with a Vytran GPX3200 device using a single direction taper process. A taper length of 4 cm was chosen to ensure adiabatic conditions throughout the process. The tapered core diameter meets the single mode criterion for splicing to the preamplifier delivery fiber.

Amplification experiments. A three-stage fiber MOPA was developed for characterization and peak power scaling of the LMA fiber (Fig. 4). The seed laser consists of a 28 ps mode-locked fiber oscillator at 1030 nm wavelength. After passing two preamplifiers and a band pass filter for spectral purity, the seed pulse is coupled into the spliced tapered LMA fiber for further power amplification. The pulse picker is used to set the pulse repetition rate, and the isolator is to protect the seed source from reverse power. The pump light of a fiber-coupled 976 nm wavelength-stabilized diode is coupled with the pump clad of the LMA fiber.

The MOPA is operated with a pulse repetition rate of 250 kHz to scale the peak power. The average seed power behind the band pass filter entering the main amplifier is 39 mW, corresponding to 4.9 kW peak power. The signal light at the fiber output is coupled with a dichroic mirror for measuring the output power, whereby it passes three wedge plates to reflect a 4% fraction of power for the measurement of the spectrum, M^2, and pulse width. For this, autocorrelation (AC) traces of the main amplifier output were recorded with an autocorrelator (APE pulse check). The peak power was calculated by $P_P = 0.88 \cdot E_P/t_P$ [24] with $t_P \approx 0.65 \cdot \mathrm{FWHM}$. The factor 0.65 is the deconvolution factor of the measured autocorrelation trace for a sech^2 pulse shape. The AC traces were recorded for the entire power range investigated. It is observed that the AC traces above 2 MW slightly change their width and shape. Up

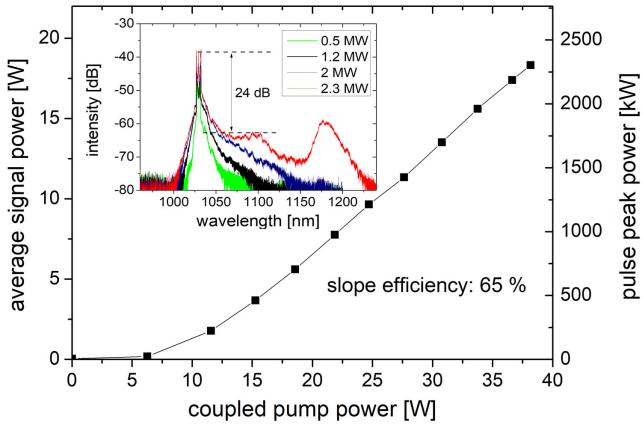

Fig. 5. Characteristics of the LMA fiber showing slope efficiency, average and peak power; output spectra are plotted in the inset.

to 2 MW, the measured full width at half maximum remains generally constant at 42 ps, which corresponds to a pulse width of 28 ps.

In Fig. 5, the average output power is plotted versus launched pump power and could be increased up to 18.3 W, which corresponds to a peak power of approximately 2.3 MW and an amplification of 26.7 dB. The slope efficiency is 65%. The emission spectra of the main amplifier are plotted in the inset of Fig. 5.

Up to a peak power of 2 MW, the spectra show a slight broadening due to stimulated Raman scattering (SRS), which however remains at a notably low power level. Above 2 MW peak power, the spectra strongly broaden, and a new peak near 1180 nm indicates the increasing influence of nonlinear processes, e.g., SRS and four-wave-mixing (FWM).

In Fig. 6 the measured M^2 values are plotted versus peak power. On average, the beam quality remains generally constant at $M^2 = 1.3$, which is a notably good result for a tapered multimode fiber. The threshold-like increase of the M^2 values from $M^2 = 1.3$ to $M^2 > 3$ is a clear indication of the rise of higher order modes (HOM). By measuring the beam quality at a higher repetition rate of 512 kHz and same average power (Fig. 6, blue and green symbols), it could be proved that it is not TMI that

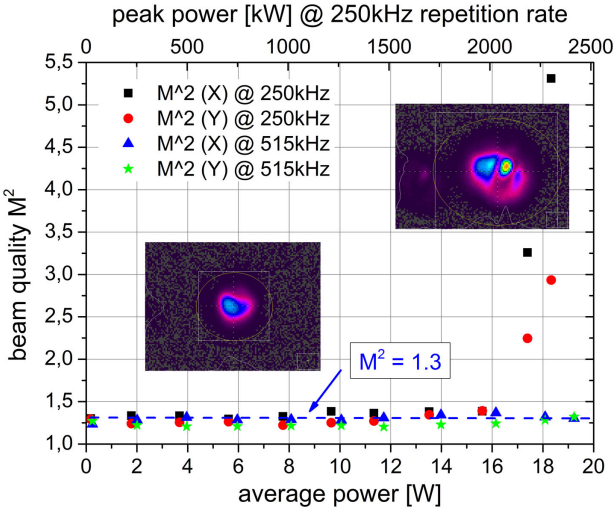

Fig. 6. Beam quality characterization: measured M^2 values for increasing peak power at different repetition rates.

occurs when a critical average power is exceeded [25]. In this case, the measured beam quality stays constant at $M^2 = 1.3$. The degradation of beam quality may be caused by different highly nonlinear effects near the damage threshold of the fiber. This is also confirmed by the strong spectral broadening above 2 MW peak power and the emission peak occurring at 1180 nm. The origin could be SRS and FWM from higher order modes, but this needs further investigation.

Conclusion. We have demonstrated a tapered fluorine codoped REPUSIL based Yb amplifier with 2 MW peak power and near diffraction-limited beam quality of $M^2 = 1.3$.

We have shown that Yb-doped REPUSIL core glass, whose RI is partially compensated by fluorine, is ideally suited for high peak power amplification. It turns out that for fundamental mode excitation in step-index LMA-fibers, the homogeneity and the symmetry of inhomogeneities of the core RI are highly important, and even small deviations can result in a visible deformed intensity distribution of the FM. Nevertheless, our experiments demonstrate near diffraction-limited beam quality and a record value of peak power for a tapered fiber amplifier, showing the potential for further improvement of the material homogeneity. The combination of simply structured and short step-index REPUSIL based fibers and the tapered amplifier concept offers the possibility of realizing cost-efficient monolithic high-power laser sources. Moreover, this new laser glass opens the possibility of realizing numerous innovative and cost-efficient fiber designs, from step index to PCF or even gain-guided index antiguided fibers [26], where the RI is set just below the silica level.

Funding. Bundesministerium für Bildung und Forschung (13N13683).

Acknowledgments. We thank SPI Lasers for providing the picosecond seed laser and the application of a fiber end cap and in particular Yuhtat Cho for valuable discussions of the measurement results. The IFA-100 as a basic tool for this research work was founded by the Free State of Thuringia under the project number 2015-0021.

Disclosures. The authors declare no conflicts of interest.

REFERENCES

1. X. Ma, C. Zhu, I.-N. Hu, A. Kaplan, and A. Galvanauskas, Opt. Express **22**, 9206 (2014).
2. F. Kong, G. Gu, T. W. Hawkins, J. Parsons, M. Jones, C. Dunn, M. T. Kalichevsky-Dong, K. Wei, B. Samson, and L. Dong, Opt. Express **21**, 32371 (2013).
3. G. R. Hadley, J. G. Fleming, and S.-Y. Lin, Opt. Lett. **29**, 809 (2004).
4. J. Limpert, F. Stutzki, F. Jansen, H. J. Otto, T. Eidam, C. Jauregui, and A. Tünnermann, Light Sci. Appl. **1**, e8 (2012).
5. A. Benoît, R. Dauliat, R. Jamier, G. Humbert, S. Grimm, K. Schuster, F. Salin, and P. Roy, Opt. Lett. **39**, 4561 (2014).
6. K. Bobkov, A. Andrianov, M. Koptev, S. Muravyev, A. Levchenko, V. Velmiskin, S. Aleshkina, S. Semjonov, D. Lipatov, A. Guryanov, A. Kim, and M. Likhachev, Opt. Express **25**, 26958 (2017).
7. Y. Zhu, M. Leich, M. Lorenz, T. Eschrich, C. Aichele, J. Kobelke, H. Bartelt, and M. Jäger, Opt. Express **26**, 17034 (2018).
8. M. F. Ando, O. Benzine, Z. Pan, J.-L. Garden, K. Wondraczek, S. Grimm, K. Schuster, and L. Wondraczek, Sci. Rep. **8**, 5394 (2018).
9. S. Jetschke, S. Unger, A. Schwuchow, M. Leich, and M. Jäger, Opt. Express **24**, 13009 (2016).
10. W. He, M. Leich, S. Grimm, J. Kobelke, Y. Zhu, H. Bartelt, and M. Jäger, Laser Phys. Lett. **12**, 015103 (2015).
11. C. Gaida, F. Stutzki, F. Jansen, H.-J. Otto, T. Eidam, C. Jauregui, O. de Vries, J. Limpert, and A. Tünnermann, Opt. Lett. **39**, 209 (2014).
12. A. Mühlich, K. Rau, F. Simmat, and N. Treber, presented at First European Conference on Optical Fiber Communication, London (1975).
13. J. W. Fleming and D. L. Wood, Appl. Opt. **22**, 3102 (1983).
14. K. Schuster, S. Grimm, A. Kalide, J. Dellith, M. Leich, A. Schwuchow, A. Langner, G. Schötz, and H. Bartelt, Opt. Mater. Express **5**, 887 (2015).
15. H. El Hamzaoui, G. Bouwmans, A. Cassez, L. Bigot, B. Capoen, M. Bouazaoui, O. Vanvincq, and M. Douay, Opt. Lett. **42**, 1408 (2017).
16. W. Xu, Z. Lin, M. Wang, S. Feng, L. Zhang, Q. Zhou, D. Chen, L. Zhang, S. Wang, C. Yu, and L. Hu, Opt. Lett. **41**, 504 (2016).
17. K. Schuster, S. Unger, C. Aichele, F. Lindner, S. Grimm, D. Litzkendorf, J. Kobelke, J. Bierlich, K. Wondraczek, and H. Bartelt, Adv. Opt. Technol. **3**, 447 (2014).
18. M. Leich, F. Just, A. Langner, M. Such, G. Schötz, T. Eschrich, and S. Grimm, Opt. Lett. **36**, 1557 (2011).
19. J. Kirchhof and S. Unger, J. Non-Cryst. Solids **354**, 540 (2008).
20. F. Froehlich, C. Aichele, S. Grimm, and K. Schuster, Opt. Mater. Express **3**, 1839 (2013).
21. J. Kirchhof, S. Unger, and J. Dellith, Opt. Mater. Express **8**, 2559 (2018).
22. F. Just, H.-R. Müller, S. Unger, J. Kirchhof, V. Reichel, and H. Bartelt, J. Lightwave Technol. **27**, 2111 (2009).
23. V. Reichel, H. Baierl, A. Kalide, A. Scheffel, J. Dellith, and K. Schuster, Proc. SPIE **10**, 105280T (2018).
24. RP Photonics Consulting GmbH, https://www.rp-photonics.com/peak_power.html.
25. T. Eidam, C. Wirth, C. Jauregui, F. Stutzki, F. Jansen, H.-J. Otto, O. Schmidt, T. Schreiber, J. Limpert, and A. Tünnermann, Opt. Express **19**, 13218 (2011).
26. A. E. Siegman, Y. Chen, V. Sudesh, M. C. Richardson, M. Bass, P. Foy, W. Hawkins, and J. Ballato, Appl. Phys. Lett. **89**, 251101 (2006).